

Syntheses of new hydroxy-[3.3]orthocyclophanes as models for the galactose oxidase Tyr-Cys cofactor

Xiaoming Liu, Simon A. Barrett, Colin A. Kilner, Mark Thornton-Pett and Malcolm A. Halcrow*

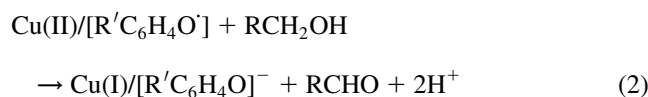
School of Chemistry, University of Leeds, Woodhouse Lane, Leeds LS2 9JT, UK

Received 29 August 2001; revised 26 October 2001; accepted 22 November 2001

Abstract—The syntheses of 3,4-benzo-8,9-(3'-hydroxybenzo)bicyclo[4,4,1]undeca-3,8-dien-11-one, 3,4-benzo-8,9-(3'-hydroxy-4'-methylsulfanylbenzo)bicyclo[4,4,1]undeca-3,8-dien-11-one and their ethylene acetals have been achieved. Crystallographic, UV/Vis and NMR data show that the two ketones adopt boat/chair conformations that are fluxional in solution, while the acetals exhibit chair/chair conformations with layered benzo rings. Comparison of the oxidation potentials of the four compounds suggests that an *ortho*-methylsulfanyl substituent and a π - π interaction both thermodynamically stabilise the phenoxonium radical species derived from these compounds, by approximately equal amounts. © 2002 Elsevier Science Ltd. All rights reserved.

1. Introduction

The fungal enzyme galactose oxidase (GOase) catalyses the aerobic oxidation of alcohols (Eq. (1)) at a copper/phenoxyl radical active site.^{1,2} The phenoxyl centre is unusually thermodynamically stable ($E_{1/2} = +0.45$ V vs NHE, vs ca. 1.0 V for a 'normal' tyrosine residue²), and can exist with a half-life as long as 1 week under certain conditions.² The Cu(II) and phenoxyl radical centres in GOase each accept one electron from the alcohol substrate (Eq. (2)), thus working in tandem to effect a two-electron oxidation.



The structure of the oxidisable tyrosinate ligand in GOase is unusual in two ways (Fig. 1).^{1,3} First, the phenol ring bears an *ortho*-thioether substituent, which is formed by a cross-linking reaction with a neighbouring cysteine residue.⁴ Second, the Tyr-Cys diamino acid moiety forms a π - π stacking interaction with a tryptophan side-chain.

Over the last five years, several groups have published model chemistry relevant to the GOase copper/radical site.⁵ The main achievements of this work to date have been the characterisation of new Cu(II)/phenoxyl complexes,^{6–11} some of which afford spectra that closely resemble that of active GOase;^{10,11} and, the preparation of

functional alcohol oxidation catalysts based on the GOase active site architecture.^{12–15} Our own work has concentrated on understanding how the unusual molecular structure of the GOase copper complex contributes to its reactivity. Using two separate series of compounds, we have demonstrated that an *ortho*-thioether substituent lowers the oxidation potential of a phenol or Cu-coordinated phenoxide ca. 0.3 V;¹¹ and, that a π - π interaction reduces the oxidation potential of an aryl radical by ca. 0.1 V, but does not contribute to its kinetic stability.¹⁶ In order to confirm these conclusions, we wished to prepare a new series of phenols containing both structural elements of the GOase phenoxyl radical in the same molecule.

In order to achieve this, we were attracted to the 3,4:8,9-dibenzobicyclo[4,4,1]undeca-3,8-dien-11-ones that have been extensively studied by Mataka and co-workers.¹⁷ These ketones exhibit boat/chair or chair/boat conformations that interconvert in solution (Scheme 1).¹⁸ However, acetalation of the ketone group causes a change to a rigid chair/chair conformation, in which the two annelated rings are stacked

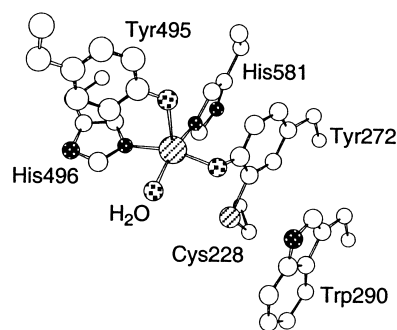
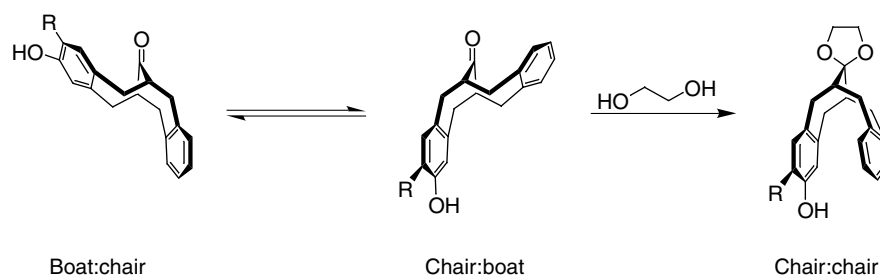


Figure 1. Crystal structure of the GOase active site.³

Keywords: synthesis; galactose oxidase; Tyr-Cys cofactor.

* Corresponding authors. Tel.: +44-113-233-6506; fax: +44-113-233-6565; e-mail: m.a.halcrow@chem.leeds.ac.uk



Scheme 1. Conformational switching of 3,4:8,9-dibenzobicyclo[4,4,1]undeca-3,8-dien-11-ones by acetalation.

above each other (Scheme 1).¹⁹ Hence, we reasoned that by preparing and comparing the four compounds in Scheme 2, we could dissect away the different structural elements of the GOase radical site. This paper describes the synthesis and spectroscopic, crystallographic and electrochemical characterisation of **1–4**. Their coordination chemistry with copper and other metal ions will be described elsewhere.

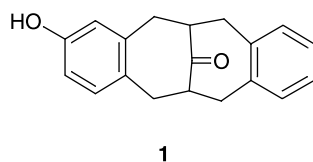
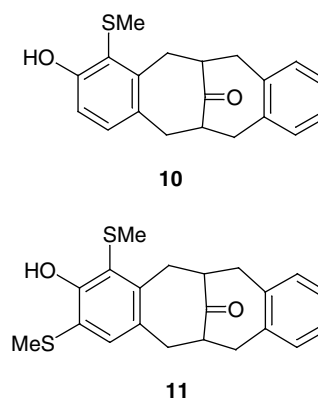
2. Results and discussion

2.1. Syntheses

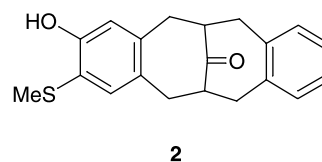
The synthesis of **1–4** is shown in Scheme 3. As we have outlined previously,²⁰ the radical bromination of 3,4-dimethylmethoxybenzene is more complex than previous literature reports imply,²¹ yielding 4-bromomethyl-3-methylmethoxybenzene²² and 4-dibromomethyl-3-methylmethoxybenzene²⁰ in addition to **6**. This distribution of products does not vary between reactions carried out over periods of 30 min–1 day. Separation of **6** from the crude mixture is arduous, involving multiple crystallisation and column chromatography steps which finally give pure **6** in 24% yield. The synthesis of **5** and the sequence of reactions converting **5** and **6** to **9** follow the Mataka methodology,¹⁹ with some modified purification procedures that afford improved yields. Deprotection of **9** in hot 48% HBr cleanly afforded **1** in 73% yield.

Compound **1** was thiomethylated by an acid-catalysed reaction with excess dimethyldisulfide.²³ Following trials using several different conditions, a solvent-free reaction

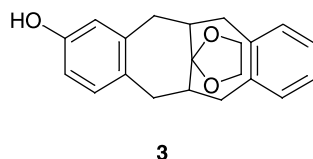
catalysed by toluenesulfonic acid monohydrate gave >90% conversion of starting material after 3 days reflux, with **2** being the dominant product. Two significant by-products, **10** and **11**, also formed in this reaction and were removed by flash column chromatography in 9:1 CH₂Cl₂/CH₃CN. Unfortunately, **10** and **11** elute very closely in this and all other solvent systems we examined. Hence, while multiple chromatographic separations did yield milligram quantities of these materials in pure form, we were unable to characterise **10** and **11** beyond confirming their identities. Interestingly, a similar reaction using the Lewis acid catalyst AlCl₃ was <50% complete after 7 days, but gave **10** rather than **2** as the major product. The reason for this difference in regioselectivity is unclear.



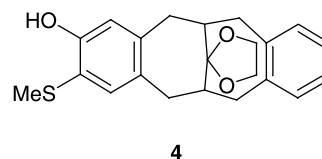
1
No thioether substituent, no π - π stack



2
Thioether substituent but no π - π stack

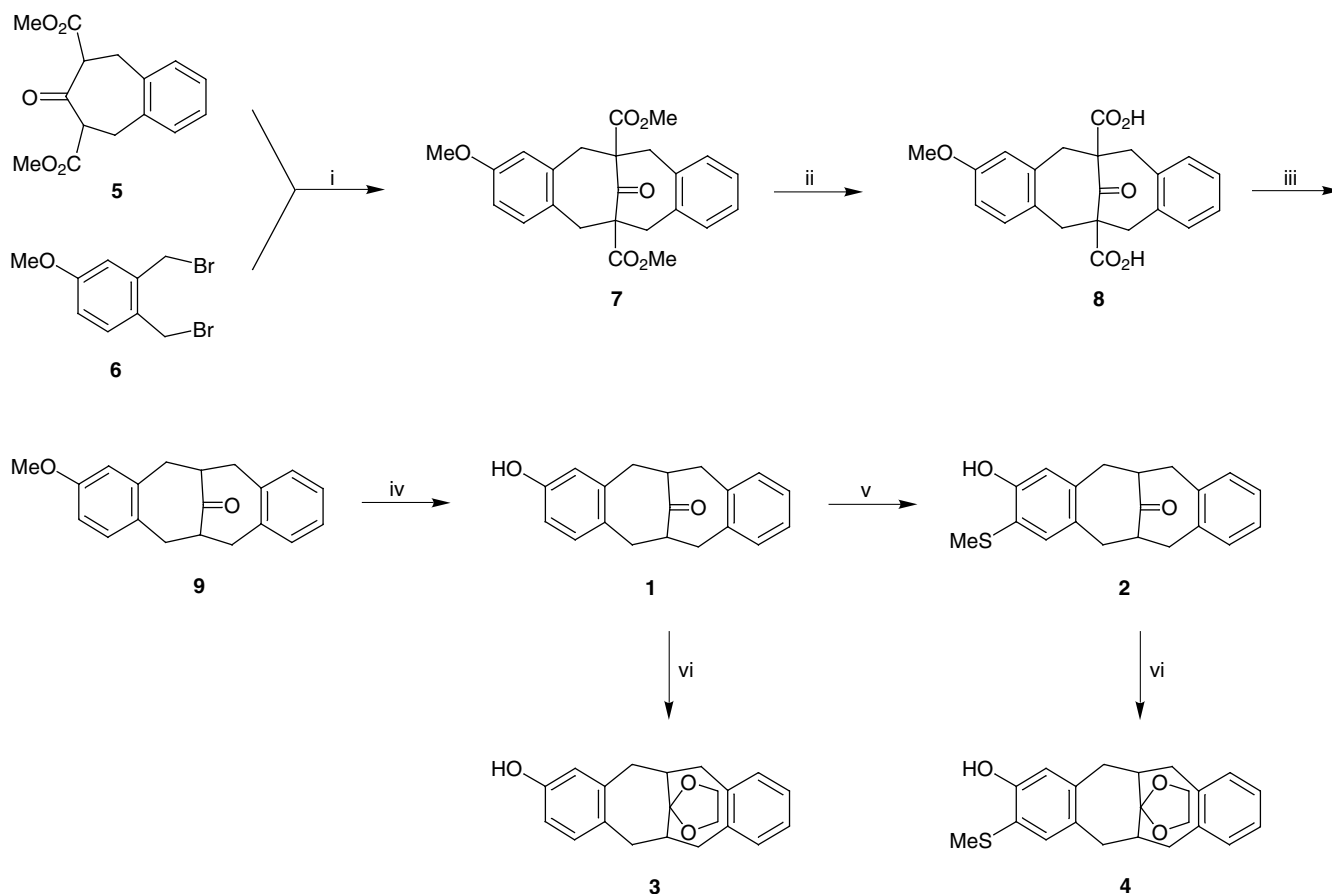


3
 π - π Stack but no thioether substituent



4
Thioether substituent and π - π stack

Scheme 2. Compounds designed as models for the GOase Tyr-Cys cofactor.



Scheme 3. (i) NBu_4Br , 5% NaOH_{aq} / CH_2Cl_2 , 6 h. (ii) KOH , EtOH , Δ , 2 h. (iii) 250°C , 30 min. (iv) 48% HBr , 120°C , 3 h. (v) MeSSMe , TsOH (cat.), Δ , 3 days. (vi) $\text{HOC}_2\text{H}_4\text{OH}$, TsOH (cat.), toluene, Δ , 24 h.

Both of these compounds exhibit a chair/boat conformation in the crystal (Figs. 2 and 3), as do all other 3,4:8,9-dibenzobicyclo[4,4,1]undeca-3,8-dien-11-ones that have been crystallographically characterised.^{18,24,25} The dihedral angles between the least squares planes of the two benzene rings are $126.88(8)^\circ$ for **1** and $128.52(9)^\circ$ for **2**, which lie within the usual range.^{18,24,25} For **1**, the hydroxyl O atom is disordered over three sites, so that 55% of the molecules in the crystal are in the boat/chair conformation, and 45% chair/boat (Scheme 1). This reproduces the relative proportions of the two conformers in solution to within experimental error (given later). The OH groups on each ring are intermolecularly hydrogen bonded to O(20) from

different neighbouring molecules, of symmetry operation $x, -y, z+1/2$ for O(21a) and $-x, -y+1, -z-1$ for O(21b) and O(21c). The packing diagram of **1** suggests that O(20) from a given molecule could accept two hydrogen bonds, from O(21a) of one neighbouring molecule and O(21b) of another. This accounts for the hydroxyl O atom not being equally distributed over the two benzyl rings of the molecule, and suggests that the distribution of phenol groups on molecules within the crystal is probably random.

In contrast to **1**, the hydroxyl and methylsulfanyl substituents of **2** are crystallographically ordered, yielding a chair/boat conformation for the molecule (Fig. 3, Scheme

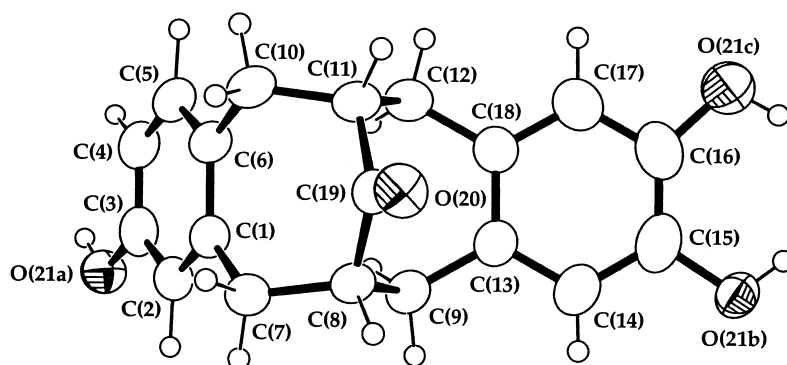


Figure 2. ORTEP drawing of **1**, showing the atom numbering scheme employed. Thermal ellipsoids are at the 50% probability level, while H atoms have arbitrary radii. The hydroxyl O atom is disordered over three sites O(21a), O(21b) and O(21c).

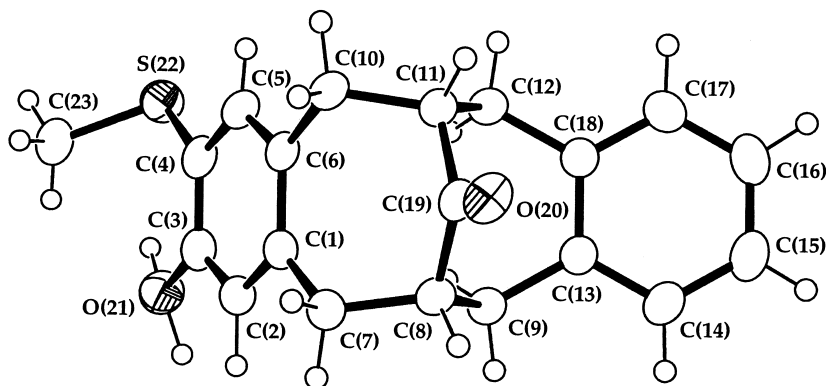


Figure 3. ORTEP drawing of **2**, showing the atom numbering scheme employed. Thermal ellipsoids are at the 50% probability level, while H atoms have arbitrary radii. The H atom bound to O(21) is disordered over two sites.

1). As is generally observed in 2-alkyl- or 2-arylsulfanylphenols,²⁶ the methylsulfanyl substituent is not coplanar with the benzo ring, the relevant torsions being C(3)–C(4)–S(22)–C(23)=54.5(3) and C(5)–C(4)–S(22)–C(23)=–131.1(2)°. The hydroxyl H atom is disordered over two orientations; one of these makes an intramolecular hydrogen bond to S(22), while the other forms an intermolecular hydrogen bond to O(20') of a neighbouring molecule related by $x+1, -y-1/2, z+1/2$.

2.3. UV/Vis and NMR spectra

The UV/Vis spectra of **1–4** were measured in CH₂Cl₂ at 293 K (Table 1). For both **1** and **2**, the longest wavelength absorption is red-shifted by 10±1 nm upon acetalation of the ketone function to form **3** or **4**. This shift is commonly observed upon conversion of [3.3]orthocyclophanes from conformationally flexible to rigid forms, and is usually attributed to the introduction of a π – π interaction between the two aromatic rings.^{19,27} The introduction of the methyl-

sulfanyl substituent in **2** and **4** also raises the wavelength of this same band by 10±1 nm. These two contributions are additive in nature, so that the highest wavelength absorption band for **4** lies at 20 nm longer wavelength compared to **1**.

The ¹H and ¹³C NMR spectra of **1–4** in CDCl₃ exhibit the expected number of peaks. Characteristically, all the aromatic H resonances of **3** and **4** lie 0.4–0.5 ppm upfield of the corresponding peaks in **1** and **2** (Table 2), which is consistent with the increased inter-arene interactions expected for the chair/chair conformations of the acetal derivatives (Scheme 1).^{19,27–29} Upon cooling the solutions of **1** and **2** to 223 K, complete decoalescence of the ¹H spectra take place owing to freezing out of the boat/chair↔chair/boat equilibrium (Scheme 1; Table 2).¹⁸ Since the H atoms on the hydroxybenzo ring resonate slightly upfield in the boat/chair form compared to the chair/boat,²⁸ it can be determined that the boat/chair conformation is favoured over the chair/boat for both **1** and **2**, by a ratio of 0.54(1):0.46(1) at 223 K in CDCl₃.¹⁷

Unexpectedly, the ¹H NMR spectra of **3** and **4** are also temperature-dependent. Although the spectra are sharp and well-defined at 298 K, at 223 K all the aliphatic and aromatic resonances have broadened although, with one exception (H_e of **4**, Scheme 4) their chemical shifts are almost identical at the two temperatures (Table 2). Unfortunately, cooling the compounds in CDCl₃ to 213 K, or of CD₂Cl₂ solutions to 180 K, simply results in further broadening of the spectra with no decoalescence being observed.

Table 1. UV/Vis spectra (CH₂Cl₂, 293 K) and electrochemical data (CH₂Cl₂/0.5 M NBu₄⁺BF₄⁻, 298 K, $\nu=0.1$ V s⁻¹) of **1–4**

	λ_{\max} , (nm) (ϵ_{\max} , 10 ³ M ⁻¹ cm ⁻¹)	Ep _a (V)
1	279 (1.9), 286 (1.8)	+1.01
2	256 (sh), 295 (5.9)	+0.70, +0.68 ^a
3	262 (5.2), 270 (7.0), 288 (4.6), 295 (sh)	+0.72
4	263 (sh), 275 (2.8), 306 (2.7)	+0.55, +0.52 ^a

^a $\nu=1.0$ V s⁻¹, $E_{1/2}$ value quoted.

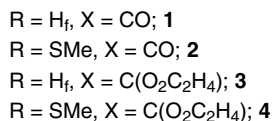
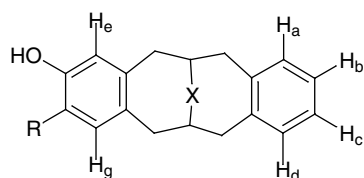
Table 2. Selected ¹H NMR data for **1–4** (500 MHz, CDCl₃). The atom labels employed are given in Scheme 4

	<i>T</i> (K)	H _{a,b,c,d}	H _e	H _f	H _g	SCH ₃	OH
1	298	7.16 (br s)	6.67 (br s)	6.60 (br d, 6.5)	7.02 (br d, 7.3)		– ^a
	233	7.11–7.32 (m)	6.49 (d, 2.4) ^b 6.80 (d, 2.1) ^c	6.36 (dd, 8.1, 2.4) ^b 6.72 (dd, 8.1, 2.1) ^c	6.88 (d, 8.1) ^b 7.15 (d, 8.1) ^c		– ^{a,b} 7.08 (s) ^c
2	298	7.16 (s)	6.52 (s)		6.81 (s)	2.28 (s)	– ^a
	233	7.32 (m)	6.74 (s) ^b 6.80 (s) ^c		6.95 (s) ^b 6.99 (s) ^c	2.26 (s) ^b 2.37 (s) ^c	7.41 (s) ^b 7.19 (s) ^c
		7.12 (s)	6.80 (s) ^c		6.99 (s) ^c	2.37 (s) ^c	7.19 (s) ^c
3	298	6.75 (m), 6.70 (m)	6.18 (d, 2.7)	6.12 (dd, 8.0, 2.7)	6.55 (d, 8.0)		– ^a
	233	6.77 (br s), 6.75 (br s)	6.21 (br s)	6.15 (br s)	6.59 (br s)		4.81 (br s)
4	298	6.74 (m), 6.69 (m), 6.63 (m)	6.14 (s)		6.32 (s)	2.18 (s)	6.76 (s)
	233	6.77 (br s), 6.72 (br s), 6.67 (br s)	6.36 (br s)		6.36 (br s)	2.20 (s)	6.81 (s)

^a Not observed.

^b Boat/chair conformation (Scheme 1).

^c Chair/boat conformation (Scheme 1).



Scheme 4. Atom labels used in Table 2.

In addition, we are unaware of low-temperature NMR data being reported for other 3,4:8,9-dibenzobicyclo[4,4,1]-undeca-3,8-dien-11-one acetal derivatives or related compounds, to provide precedent for these observations. Hence, the nature of this previously unremarked fluxional process in **3** and **4** is presently uncertain.

2.4. Electrochemistry and calculations

Cyclic voltammograms (CVs) and differential pulse voltammograms (DPVs) of **1–4** were measured in CH₂Cl₂ containing 0.5 M NBu₄⁺BF₄⁻ (Table 1). All four compounds exhibit an oxidation that is irreversible at 298 K at scan rates (ν)=0.1 V s⁻¹ although, for **2** and **4** only, weak return waves with $I_p^c/I_p^a \approx 0.2$ were observed at $\nu=1.0$ V s⁻¹. At 223 K, for **4** only this oxidation became significantly more reversible, affording $I_p^c/I_p^a \approx 0.6$ at $\nu=1.0$ V s⁻¹ (Fig. 4). We attribute this improved reversibility to the potential for intramolecular O–H···S hydrogen bonding, which would hinder deprotonation of the initial oxidation products [**2**]⁺ and [**4**]⁺; and, for **4** only, to the steric protection afforded by the intramolecular π – π interaction.¹⁶

It is noteworthy that E_{p_a} of **4**, which contains both of the unusual structural elements of the GOase Tyr-Cys cofactor (Scheme 2), is 0.46 V lower than E_{p_a} of **1**, which has neither of them. This is very similar to the 0.5 V stabilisation of the Tyr-Cys radical in GOase compared to a ‘normal’ tyrosyl radical.² Comparison of the CVs of **1–4** implies that a methylsulfanyl substituent and a π – π interaction both act to lower the oxidation potential of the phenol ring in these compounds, by similar but somewhat variable amounts. In

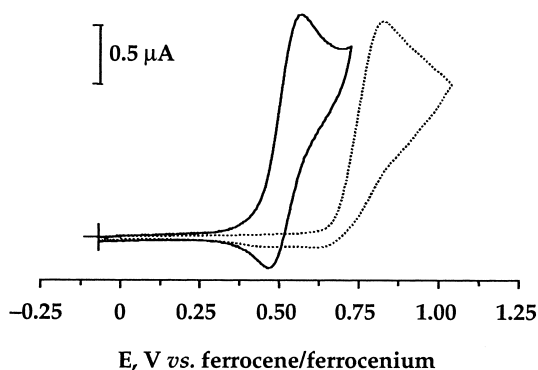


Figure 4. Cyclic voltammograms of **3** (dotted line) and **4** (solid line) at 223 K in CH₂Cl₂/0.5 M NBu₄⁺BF₄⁻ at $\nu=1.0$ V s⁻¹.

particular, the differences between E_{p_a} for **1** and **3** (0.29 V), and for **2** and **4** (0.15 V), imply that the π – π interaction contributes substantially more to the thermodynamic stability of the oxidised species than we¹⁶ or others³⁰ have previously found in other systems. However, an alternative explanation for these data could be that the identity of the bridgehead group (i.e. carbonyl or acetal function) has an effect on the π -orbital energies. This suggestion has been made previously,¹⁷ but has not yet been quantified.

In order to investigate whether the acetal moiety in **3** and **4** might contribute to their π -electronic structure, semi-empirical PM3 calculations³¹ were carried out on **1** and **3** in the chair/chair conformation (Scheme 1). The relative disposition of the benzo groups in both energy-minimised structures are identical to within experimental error, with the dihedral angle between the planes of the two benzo groups being $26 \pm 1^\circ$, and the shortest inter-arene C–C distance being 3.03 ± 0.01 Å. These parameters agree well with the crystallographic structures of other [3.3]orthocyclophanes with a chair/chair conformation.^{19,25,27,32} The HOMOs of both compounds have π -character, and are localised predominantly on the hydroxybenzo ring. The calculated HOMO energies for the two compounds are -8.96 eV for **1** and -8.70 eV for **3**, showing that at this level of theory $E_{p_a}\{\mathbf{3}\} < E_{p_a}\{\mathbf{1}, \text{chair/chair}\}$ by 0.26 V. Hence, although relative orbital energies derived semi-empirically are not especially accurate,³³ this preliminary study shows it is feasible that the identity of the bridgehead substituent might significantly perturb the π -orbital energies of these compounds. A more detailed *ab initio* study of the conformational and electronic structures of these molecules is in progress, and will be reported separately.

3. Conclusions

The hydroxy-[3.3]orthocyclophanes **1–4** have been prepared, and shown to exhibit the same conformational properties as other known 3,4:8,9-dibenzobicyclo[4,4,1]-undeca-3,8-dien-11-ones and their acetals.¹⁷ Hence, **1** and **2** exhibit boat/chair conformations that are fluxional in solution, while **3** and **4** adopt chair/chair conformations with stacked benzo rings. However, NMR data show that **3** and **4** exhibit a low-energy fluxional process that has not been detected before, and whose nature is uncertain. Compound **4** exhibits an oxidation potential 0.46 V lower than that of **1**. This mirrors almost exactly the thermodynamic stabilisation of the GOase Tyr-Cys phenoxy radical, which contains an *ortho*-thioether substituent and an overlying π – π interaction.² Further synthetic and theoretical studies are in progress, to deconvolute the contribution made by each of these two structural features to the stabilisation of [**4**]⁺.

4. Experimental

4.1. Materials

Unless otherwise stated, all manipulations were carried out in air using commercial grade solvents except that, prior to use, CCl₄ was distilled over P₂O₅, toluene was distilled over sodium and ethylene glycol was dried over activated

molecular sieves. *N*-Bromosuccinimide, benzoylperoxide, tetra-*n*-butylammonium bromide, HBr (48%), toluenesulfonic acid monohydrate, dimethyl 1,3-acetonedicarboxylate, dimethyldisulfide, 3,4-dimethylmethoxybenzene and 1,2-*bis*(bromomethyl)benzene were used as supplied.

4.2. General

Infra-red spectra were obtained as Nujol mulls pressed between NaCl windows between 400–4000 cm^{-1} using a Nicolet Avatar 360 spectrophotometer. UV/Vis spectra were obtained with a Perkin–Elmer Lambda 900 spectrophotometer operating between 3300–200 nm, in 1 cm quartz cells. All room temperature NMR spectra were run on a Bruker ARX250 spectrometer, operating at 250.1 MHz (^1H) and 62.9 MHz (^{13}C). Variable temperature NMR spectra of **1–4** were run on a Bruker DRX500 spectrometer, operating at 500.1 MHz (^1H) and 125.8 MHz (^{13}C). FAB mass spectra were performed on a VG AutoSpec spectrometer, employing a 3-NOBA matrix. CHN microanalyses were performed by the University of Leeds School of Chemistry microanalytical service. Melting points are uncorrected. Semi-empirical calculations were carried out using the CHEM3D molecular modelling suite.³⁴ A preliminary conformational search was first carried out using the MM2 molecular mechanics package,³⁵ and the chosen conformation then refined at the restricted Hartree–Fock PM3 level.³⁶

All electrochemical measurements employed an AUTO-LAB PGSTAT 30 potentiostat, using a conventional three-electrode electrochemical cell under an Ar atmosphere. Measurements were carried out in CH_2Cl_2 containing 0.5 M $\text{NBu}_4^+\text{BF}_4^-$ as supporting electrolyte. The working electrode was a Pt wire (0.5 mm in diameter) embedded in a glass tube, while a Pt rod counter electrode and AgCl/Ag reference electrode were used. All potentials quoted are referenced to an internal ferrocene/ferrocenium standard and were obtained at a scan rate of 100 mV s^{-1} , unless otherwise stated.

4.3. Syntheses

4.3.1. Dimethyl 3-oxo-1,2,4,5-tetrahydrobenzo[*d*]-cycloheptene-2,4-dicarboxylate (5). A modification of the literature procedure was used.¹⁹ NBu_4^+Br (18.1 g, 56 mmol) was dissolved in a mixture of aqueous 5% NaHCO_3 (780 cm^3) and CH_2Cl_2 (75 cm^3) in three-neck flask equipped with mechanical stirrer. A solution of 1,2-*bis*(bromomethyl)benzene (24.8 g, 94 mmol) and dimethyl 1,3-acetonedicarboxylate (30.5 g, 170 mmol) in CH_2Cl_2 (240 cm^3) was added dropwise to this mixture, with vigorous stirring. The mixture was then stirred for a further 36 h at room temperature. The organic layer was separated, dried over Na_2SO_4 and evaporated to dryness. The red residue was crystallised from 2:1 EtOH/hexanes at -30°C , yielding a white solid that was isolated and washed with cold EtOH. The product was recrystallised from hot EtOH. Yield 16.4 g, 63%. Found: C, 65.3; H, 5.9%. Calcd for $\text{C}_{15}\text{H}_{16}\text{O}_5$: C, 65.2; H, 5.8%. Mp 102–109°C (lit. 103–110°C¹⁹).

4.3.2. 3,4-Bis(bromomethyl)methoxybenzene (6). To a

solution of 3,4-dimethylmethoxybenzene (12.0 g, 88 mmol) in CCl_4 (120 cm^3) was added *N*-bromosuccinimide (34.6 g, 190 mmol) and benzoylperoxide (0.10 g, 0.47 mmol). The mixture was refluxed for 30 min and allowed to cool. The solution was filtered, and the filtrate evaporated to dryness. The resultant brown oil was dissolved in 1:1 Et_2O /hexanes and stored at -30°C , yielding white moisture-sensitive crystals of 4-dibromomethyl-3-methylmethoxybenzene that were removed by filtration.²⁰ This crystallisation procedure was repeated until none of this contaminant remained by TLC. The remaining oil was purified by silica flash chromatography (CH_2Cl_2 eluent) to give a colourless oil, which formed white needles from Et_2O /hexanes. These were collected, washed with hexanes, dried in vacuo and stored at -30°C . Yield 6.2 g, 24%. Found: C, 36.7; H, 3.5%. Calcd for $\text{C}_9\text{H}_{10}\text{OBr}_2$: C, 36.8; H, 3.4%. Mp 46–48°C (lit. 49–50°C²¹).

4.3.3. Dimethyl 11-oxo-3,4-benzo-8,9-(3'-methoxybenzo)-bicyclo[4.4.1]undeca-3,8-dien-1,6-dicarboxylate (7). Tetra-butylammonium bromide (1.9 g, 6.0 mmol) was added dropwise to a mixture of aqueous NaOH (5%, 50 cm^3) and CH_2Cl_2 (20 cm^3). With vigorous stirring, a CH_2Cl_2 (50 cm^3) solution of **5** (2.8 g, 10.0 mmol) and **6** (2.9 g, 10.0 mmol) was added dropwise to this mixture, which was then stirred for a further 6 h. The organic layer was separated, washed with water (2×50 cm^3) and dried over Na_2SO_4 . Removal of the solvent yielded a sticky paste, which was purified by silica flash chromatography (9:1 $\text{CH}_2\text{Cl}_2/\text{CH}_2\text{CN}$, eluent) to yield a white solid. Yield 3.3 g, 81%. Found: C, 69.6, H, 6.0%. Calcd for $\text{C}_{24}\text{H}_{24}\text{O}_6$: C, 70.6, H, 5.9%. Mp 93–95°C. Mass spectrum: $m/z=408$ [M]⁺. ^1H NMR (CDCl_3): 7.14–7.26 (br m, 5H), 6.82 (br s, 1H), 6.73 (br s, 1H), 3.78 (s, 3H), 3.75 (s, 6H), 3.37–3.65 (br m, 4H), 2.74–3.12 (br m, 6H). ^{13}C NMR (CDCl_3): δ 206.3, 173.0 (2C), 159.0 (br), 138.2 (br), 137.1 (br), 134.1 (br), 131.8 (br), 130.5 (br), 129.2 (br), 128.6 (br), 127.1 (br), 118.0 (br), 116.0 (br), 112.4 (br), 64.1, 64.0, 55.3, 52.3 (2C), 39.9 (br, 2C), 35.7 (br, 2C). IR (nujol): 1738, 1694 cm^{-1} .

4.3.4. 11-Oxo-3,4-benzo-8,9-(3'-methoxybenzo)bicyclo[4.4.1]undeca-3,8-dien-1,6-dicarboxylic acid (8). A suspension of **7** (2.0 g, 4.9 mmol) and KOH (7.0 g, 130 mmol) in EtOH (60 cm^3) was refluxed for 2 h. After cooling to room temperature, the mixture was diluted with water (300 cm^3) and neutralised with 3 M HCl. A pale yellow precipitate formed, which was collected and washed sequentially with water and ethanol (10 cm^3) to leave a white solid. Yield 1.3 g, 70%. Found: C, 69.5; H, 5.4%. Calcd for $\text{C}_{22}\text{H}_{20}\text{O}_6$: C, 69.5, H 5.3%. Mp 274°C dec. Mass spectrum: $m/z=380$ [M]⁺. ^1H NMR ($\{\text{CD}_3\}_2\text{SO}$): δ 12.60 (s, 2H), 7.18 (br s, 5H), 6.77–6.85 (br m, 2H), 3.70 (s, 3H), 3.35 (br s, 2H), 2.92 (br s, 8H). ^{13}C NMR ($\{\text{CD}_3\}_2\text{SO}$): δ 206.9, 173.9, 173.8, 158.7 (br), 138.8 (br), 137.7 (br, 2C), 132.4 (br), 131.4 (br, 2C), 129.4 (br), 127.3 (br, 2C), 117.8 (br), 112.9 (br), 63.6, 63.5, 55.3 (CH_2 peaks obscured by solvent). IR (nujol): 1710, 1688 cm^{-1} .

4.3.5. 3,4-Benzo-8,9-(3'-methoxybenzo)bicyclo[4.4.1]undeca-3,8-dien-11-one (9). Solid **8** (5.9 g, 15.5 mmol) was heated at 250°C for 30 min under N_2 . After cooling to room temperature, the residue was dissolved in CH_2Cl_2 (100 cm^3). Insoluble material was filtered off and the solvent

Table 3. Experimental details for the single crystal structure determinations in this study

	1	2
Formula	C ₁₉ H ₁₈ O ₂	C ₂₀ H ₂₀ O ₂ S
M _r	278.33	324.42
Crystal habit	Colourless block	Colourless plate
Crystal size (mm)	0.33×0.23×0.15	0.38×0.26×0.04
Crystal system, space group	Orthorhombic, <i>Pbcn</i>	Monoclinic, <i>P2₁/c</i>
<i>a</i> (Å)	15.2693(5)	10.6189(5)
<i>b</i> (Å)	11.4670(3)	12.9759(7)
<i>c</i> (Å)	16.3840(4)	14.1304(6)
β (°)	–	123.798(3)
<i>V</i> (Å ³)	2868.72(14)	1617.98(13)
<i>Z</i>	8	4
μ (mm ⁻¹)	0.082	0.208
ρ _{calc} (mg m ⁻³)	1.289	1.332
<i>T</i> (K)		150(2)
Diffractometer		Nonius KappaCCD
Radiation		Graphite-monochromated Mo K _α
λ (Å)		0.71073
Scan type		Area detector scans
Measured reflections	30,773	8928
Independent reflections	3287	3532
<i>R</i> _{int}	0.068	0.049
Absorption correction		Multi-scan
Min. transmission	0.97	0.93
Max. transmission	0.99	0.99
Observed reflections [<i>I</i> >2σ(<i>I</i>)]	2420	2848
Range in 2θ (°)	4.4≤2θ≤55.0	6.0≤2θ≤54.9
Range in <i>h</i>	–19≤ <i>h</i> ≤19	–13≤ <i>h</i> ≤13
Range in <i>k</i>	–13≤ <i>k</i> ≤14	–16≤ <i>k</i> ≤15
Range in <i>l</i>	–21≤ <i>l</i> ≤18	–18≤ <i>l</i> ≤88
Completeness to 2θ _{max}	0.999	0.953
No. of parameters	264	284
<i>R</i> (<i>F</i>) ^a , <i>wR</i> (<i>F</i> ²) ^b	0.060, 0.150	0.064, 0.169
GOF	1.160	1.058
Weighting scheme ^c	$w=1/[\sigma^2(F_o^2)+(0.0349P)^2+2.0892P]$	$w=1/[\sigma^2(F_o^2)+(0.0613P)^2+1.9489P]$
Max. shift/e.s.d	<0.001	<0.001
Δρ _{min} , Δρ _{max} (e Å ⁻³)	–0.16, 0.20	–0.41, 0.61

$$^a R = \frac{\sum ||F_o| - |F_c||}{\sum |F_o|}$$

$$^b wR = \left[\frac{\sum w(F_o^2 - F_c^2)^2}{\sum wF_o^4} \right]^{1/2}$$

$$^c P = (F_o^2 + 2F_c^2)/3$$

was removed. The resultant white solid was washed with Et₂O and dried in vacuo. The product was recrystallised from CH₂Cl₂/Et₂O. Yield 4.2 g, 93%. Found: C, 82.0, H, 7.0%. Calcd for C₂₀H₂₀O₂: C, 82.2, H, 6.9%. Mp 115–118°C. Mass spectrum: *m/z*=292 [M]⁺. ¹H NMR (CDCl₃): δ 7.16 (s, 4H), 7.09 (d, 8.1 Hz, 1H), 6.75 (s, 1H), 6.71 (d, 8.1 Hz, 1H), 3.78 (s, 3H), 3.07–3.19 (br m, 2H), 2.80–2.93 (br m, 8H). ¹³C NMR (CDCl₃): δ 215.3, 158.7, 139.5, 138.3, 138.2, 131.4 (br), 130.3 (br), 130.1 (br), 127.2, 127.2, 116.7 (br), 111.6 (2C), 55.2, 53.5, 53.4, 35.0 (br, 4C). IR (nujol): 1691 cm⁻¹.

4.3.6. 3,4-Benzo-8,9-(3'-hydroxybenzo)bicyclo[4,4,1]-undeca-3,8-dien-11-one (1). A suspension of **9** (9.4 g, 32 mmol) was suspended in 48% HBr (100 cm³) and heated at 120°C for three hours. The mixture was cooled to room temperature, and the resultant pink precipitate was collected, washed with water and dried over P₂O₅ in vacuo. The crude solid was washed twice with hot MeCN, to yield an off-white solid which was recrystallised from hot MeOH. Yield 6.50 g, 73%. Found: C, 81.7, H, 6.5%. Calcd for C₁₉H₁₈O₂: C, 82.0, H, 6.5%. Mp 214–216°C. Mass spectrum: *m/z*=278 [M]⁺. ¹H NMR (CDCl₃): δ 7.16 (s, 4H), 7.01 (d, 8.0 Hz, 1H), 6.66 (s, 1H), 6.60 (d, 8.0 Hz, 1H), 3.09–3.16 (m, 2H), 2.77–2.89 (m, 8H). ¹³C NMR (CDCl₃): δ 215.7, 154.7, 139.7, 138.2, 138.1, 131.1 (br),

130.4 (br), 130.2, 127.3, 127.3, 117.8 (br), 113.6 (2C), 53.5, 53.4, 35.3 (br, 4C). IR (nujol): 3338, 1699, 1683 cm⁻¹.

4.3.7. 3,4-Benzo-8,9-(3'-hydroxy-4'-methylsulfanylbenzo)-bicyclo[4,4,1]undeca-3,8-dien-11-one (2), 3,4-benzo-8,9-(3'-hydroxy-2'-methylsulfanylbenzo)bicyclo[4,4,1]undeca-3,8-dien-11-one (10) and 3,4-benzo-8,9-(3'-hydroxy-2',4'-bis{methylsulfanyl}benzo)bicyclo[4,4,1]undeca-3,8-dien-11-one (11). Compound **1** (2.8 g, 10.0 mmol) and toluenesulfonic acid monohydrate (10 mg) were dissolved in dimethyl disulfide (100 cm³). The solution was refluxed until all the starting material was consumed by TLC (ca. 3 days). The solvent was removed, and the residue was boiled with hexanes (200 cm³) overnight. The solution was filtered hot, then cooled to room temperature to yield a white solid (1.3 g). A second crop (1.6 g) was obtained by a second extraction of the residue from the first extraction, in boiling 1:1 hexanes/Et₂O. Both crops contained three distinct products by TLC, which were separated by silica flash chromatography (9:1 CH₂Cl₂/CH₃CN eluent). Compound **2** (*R_f*=0.73) can be isolated by this method, and further purified by recrystallisation from CH₂Cl₂/Et₂O. Yield 1.7 g, 52%. Repeated silica column chromatography in the same eluent allowed the purification of small amounts of **10** (*R_f*=0.82) and **11** (*R_f*=0.86), that were sufficient for their unambiguous identification. For **2**: Found: C, 74.4, H, 6.3%.

Calcd for $C_{20}H_{20}O_2S$: C, 74.0, H, 6.2%. Mp 154–157°C. Mass spectrum: $m/z=324 [M]^+$. 1H NMR ($CDCl_3$): δ 7.16 (s, 4H), 6.81 (s, 1H), 6.52 (s, 1H), 3.05–3.16 (m, 2H), 2.77–2.92 (m, 8H), 2.28 (s, 3H). ^{13}C NMR ($CDCl_3$): δ 215.0, 153.4, 141.3, 138.0, 138.0, 136.0 (br), 130.6 (2C), 127.3, 127.3, 118.9, 116.7 (br, 2C), 53.3, 53.2, 35.2 (br, 4C), 19.9. IR (nujol): 3297, 1685, 1598 cm^{-1} . For **10**: Found: C, 73.4, H, 6.1%; Calcd for $C_{20}H_{20}O_2S$: C, 74.0, H, 6.2%. Mp 167–170°C. Mass spectrum: $m/z=324 [M]^+$. 1H NMR ($CDCl_3$): δ 7.23 (s, 4H), 7.02 (d, $J=8.2$ Hz, 1H), 6.95 (br s, 1H), 6.77 (d, $J=8.2$ Hz, 1H), 2.96–3.17 (br m, 8H), 2.65–2.81 (br m, 2H), 2.16 (s, 3H). ^{13}C NMR ($CDCl_3$): δ 215.0, 155.9, 142.9, 138.0, 137.9, 131.4 (br, 3C), 130.7, 127.4, 127.4, 112.7 (2C), 53.3, 53.2, 36.4 (br, 4C), 19.6. IR (nujol): 3393, 1691, 1584 cm^{-1} . For **11**: Found: C, 68.0, H, 6.0%. Calcd for $C_{21}H_{22}O_2S_2$: C, 68.1, H, 6.0%. Mp 79–81°C. Mass spectrum: $m/z=370 [M]^+$. 1H NMR ($CDCl_3$): δ 7.28 (br s, 1H), 7.23 (s, 4H), 6.97 (s, 1H), 2.56–3.26 (br m, 10H), 2.36 (s, 3H), 2.16 (s, 3H). ^{13}C NMR ($CDCl_3$): δ 214.8, 153.8, 147.5, 140.7, 137.9, 137.8, 131.5 (br, 3C), 131.1, 127.4 (2C), 121.2, 53.2, 53.1, 36.4 (br, 4C), 19.4, 16.2. IR (nujol): 3343, 1696 cm^{-1} .

4.3.8. 3,4-Benzo-8,9-(3'-hydroxybenzo)bicyclo[4,4,1]undeca-3,8-dien-11-one ethylene acetal (3). Compound **1** (2.4 g, 86.3 mmol) and toluenesulfonic acid monohydrate (100 mg) were suspended in a mixture of toluene (120 cm^3) and ethylene glycol (24 g, 390 mmol). The mixture was refluxed under N_2 for one day, using a condenser filled with activated molecular sieves. Following removal of the solvent, the residue was crystallised from hot methanol to yield a white solid was obtained and dried in vacuum. Yield 2.0 g, 75%. Found: C, 78.3, H, 6.9%. Calcd for $C_{21}H_{22}O_3$: C, 78.2, H, 6.9%. Mp 243–245°C. Mass spectrum: $m/z=322 [M]^+$. 1H NMR ($CDCl_3$): δ 6.68–6.79 (m, 4H), 6.55 (d, $J=8.0$ Hz, 1H), 6.18 (d, $J=2.7$ Hz, 1H), 6.11 (dd, $J=8.0$, 2.7 Hz, 1H), 4.24 (br s, 1H), 4.05 (s, 4H), 3.33–3.43 (m, 4H), 2.56–2.71 (m, 4H), 2.28–2.29 (m, 2H). ^{13}C NMR ($CDCl_3$): δ 153.0, 141.1, 139.7, 139.3, 132.0, 131.5, 130.3, 130.3, 125.9, 125.2, 117.5, 113.6, 112.1, 64.5 (2C), 36.5, 36.4, 36.4, 35.4. IR (nujol): 3385, 1609 cm^{-1} .

4.3.9. 3,4-Benzo-8,9-(3'-hydroxy-4'-methylsulfonylbenzo)bicyclo[4,4,1]undeca-3,8-dien-11-one ethylene acetal (4). Method as for **3**, using **2** (0.41 g, 1.3 mmol) with the other quantities adjusted to suit. The product was a white solid that was recrystallised from hot MeOH. Yield 0.36 g, 80%. Found: C, 71.2, H, 6.3%. Calcd for $C_{22}H_{24}O_3S$: C, 71.7, H, 6.6%. Mp 148–150°C. Mass spectrum: $m/z=368 [M]^+$. 1H NMR ($CDCl_3$): 6.62–6.76 (m, 5H) 6.32 (s, 1H), 6.14, (s, 1H), 4.06 (s, 4H), 3.33–3.44 (m, 4H), 2.60–2.71 (m, 4H), 2.27–2.29 (m, 2H), 2.18 (s, 3H). ^{13}C NMR ($CDCl_3$): 153.7, 143.1, 139.7, 139.3, 136.4, 132.5, 130.6, 130.2, 126.1, 125.1, 116.9, 115.7, 113.4, 64.6 (2C), 42.6, 42.3, 36.4, 35.3, 19.3. IR (nujol): 3388, 1607, 1566 cm^{-1} .

4.3.10. Single crystal X-ray structure determinations. Single crystals of **1** were grown from slow evaporation of a solution of the compound in a mixture of CH_2Cl_2 and $CHCl_3$. Single crystals of **2** were grown from hot MeOH. Experimental details from the structure determinations are given in Table 3. Both structures were solved by direct methods (SHELXS 97³⁷) and refined by full matrix least-

squares on F^2 (SHELXL 97³⁸). For **1**, the phenolic OH group was disordered over three sites, O(21a), O(21b) and O(21c) with refined occupancies of 0.45, 0.40 and 0.15, respectively. All wholly occupied H atoms were located in the difference map and allowed to refine freely. Refined C–H distances ranged from 0.93(3)–1.09(3) Å. The six partial H atoms were placed in calculated positions and refined using a riding model. All non-H atoms except O(21c) were refined anisotropically, and no restraints were applied. For **2**, all C-bound H atoms were located in the difference map and allowed to refine freely. Two Fourier peaks were observed in the vicinity of O(21), suggesting that the phenolic H atom is disordered over two sites. The two half-occupied H atoms H(21a) and H(21b) were refined as a rigid group. Refined C–H distances ranged from 0.92(3)–1.03(3) Å. All non-H atoms were refined anisotropically, and no restraints were applied.

Crystallographic data (excluding structure factors) for the structures in this paper have been deposited with the Cambridge Crystallographic Data Centre as supplementary publication numbers 169135 (**1**) and 169136 (**2**). Copies of the data can be obtained, free of charge, on application to CCDC, 12 Union Road, Cambridge CB2 1EZ, UK [Fax: +44(0)-1223-336033 or email: deposit@ccdc.cam.ac.uk].

Acknowledgements

The authors thank the EPSRC (X. L.) and the Royal Society of London (M. A. H.) for funding.

References

- Halcrow, M. A.; Phillips, S. E. V.; Knowles, P. F. *Subcell. Biochem.* **2000**, *35*, 183–231.
- Whittaker, J. W.; Whittaker, M. M. *Pure Appl. Chem.* **1998**, *70*, 903–910.
- Ito, N.; Phillips, S. E. V.; Stevens, C.; Ogel, Z. B.; McPherson, M. J.; Keen, J. N.; Yadev, K. D. S.; Knowles, P. F. *Nature (London)* **1991**, *350*, 87–90.
- Halcrow, M. A. *Angew. Chem., Int. Ed. Engl.* **2001**, *40*, 346–349.
- Jazdzewski, B. A.; Tolman, W. B. *Coord. Chem. Rev.* **2000**, *200–202*, 633–685.
- Halfen, J. A.; Young Jr., V. G.; Tolman, W. B. *Angew. Chem., Int. Ed. Engl.* **1996**, *35*, 1687–1690. Halfen, J. A.; Jazdzewski, B. A.; Mahaptara, S.; Berreau, L. M.; Wilkinson, E. C.; Que Jr., L.; Tolman, W. B. *J. Am. Chem. Soc.* **1997**, *119*, 8217–8227.
- Zurita, D.; Gautier-Luneau, I.; Ménage, S.; Pierre, J.-L.; Saint-Aman, E. *J. Biol. Inorg. Chem.* **1997**, *2*, 46–55.
- Sokolowski, A.; Leutbecher, H.; Weyhermüller, T.; Schnepf, R.; Bothe, E.; Bill, E.; Hildenbrandt, P.; Wieghardt, K. *J. Biol. Inorg. Chem.* **1997**, *2*, 444–453. Müller, J.; Weyhermüller, T.; Bill, E.; Hildenbrandt, P.; Ould-Moussa, L.; Glaser, T.; Wieghardt, K. *Angew. Chem., Int. Ed. Engl.* **1998**, *37*, 616–619.
- Itoh, S.; Takayama, S.; Arakawa, R.; Furuta, A.; Komatsu, M.; Ishida, A.; Takamuku, S.; Fukuzumi, S. *Inorg. Chem.* **1997**, *36*, 1407–1416.
- Itoh, S.; Taki, M.; Kumei, H.; Takayama, S.; Nagamoto, S.;

- Kitagawa, T.; Sakurada, N.; Arakawa, R.; Fukuzumi, S. *Inorg. Chem.* **2000**, *39*, 3708–3711. Taki, M.; Kumei, H.; Nagamoto, S.; Kitagawa, T.; Itoh, S.; Fukuzumi, S. *Inorg. Chim. Acta* **2000**, *300–302*, 622–632.
11. Halcrow, M. A.; Chia, L. M. L.; Liu, X.; McInnes, E. J. L.; Yellowlees, L. J.; Mabbs, F. E.; Davies, J. E. *Chem. Commun.* **1998**, 2465–2466. Halcrow, M. A.; Chia, L. M. L.; Liu, X.; McInnes, E. J. L.; Yellowlees, L. J.; Mabbs, F. E.; Scowen, I. J.; McPartlin, M.; Davies, J. E. *J. Chem. Soc., Dalton Trans.* **1999**, 1753–1762.
12. Wang, Y.; Stack, T. D. P. *J. Am. Chem. Soc.* **1996**, *118*, 13097–13098. Wang, Y.; DuBois, J. L.; Hedman, B.; Hodgson, K. O.; Stack, T. D. P. *Science* **1998**, *279*, 537–540. Mahadevan, V.; Gebbink, R. J. M. K.; Stack, T. D. P. *Curr. Opin. Chem. Biol.* **2000**, *4*, 228–234.
13. Chaudhuri, P.; Hess, M.; Flörke, U.; Wieghardt, K. *Angew. Chem., Int. Ed. Engl.* **1998**, *37*, 2217–2220. Chaudhuri, P.; Hess, M.; Weyhermüller, T.; Wieghardt, K. *Angew. Chem., Int. Ed. Engl.* **1999**, *38*, 1095–1098. Chaudhuri, P.; Hess, M.; Müller, J.; Hildenbracht, K.; Bill, E.; Weyhermüller, T.; Wieghardt, K. *J. Am. Chem. Soc.* **1999**, *121*, 9599–9610.
14. Saint-Aman, E.; Ménage, S.; Pierre, J.-L.; Defrancq, E.; Gelion, G. *New J. Chem.* **1998**, *22*, 393–394.
15. Itoh, S.; Taki, M.; Takayama, S.; Nagamoto, S.; Kitagawa, T.; Sakurada, N.; Arakawa, R.; Fukuzumi, S. *Angew. Chem., Int. Ed. Engl.* **1999**, *38*, 2774–2776. Taki, M.; Kumei, H.; Itoh, S.; Fukuzumi, S. *J. Inorg. Biochem.* **2000**, *78*, 1–5.
16. Halcrow, M. A.; McInnes, E. J. L.; Mabbs, F. E.; Scowen, I. J.; McPartlin, M.; Powell, H. R.; Davies, J. E. *J. Chem. Soc., Dalton Trans.* **1997**, 4025–4035. Liu, X.; Chia, L. M. L.; Kilner, C. A.; Yellowlees, L. J.; Thornton-Pett, M.; Trofimenko, S.; Halcrow, M. A. *Chem. Commun.* **2000**, 1947–1948.
17. Mataka, S.; Thiemann, T.; Taniguchi, M.; Sawada, T. *Synlett* **2000**, 1211–1227.
18. Mataka, S.; Takahashi, K.; Hirota, T.; Takuma, K.; Kobayashi, H.; Tashiro, M.; Imada, K.; Kuniyoshi, M. *J. Org. Chem.* **1986**, *51*, 4618–4622.
19. Mataka, S.; Takahashi, K.; Mimura, T.; Hirota, T.; Takuma, K.; Kobayashi, H.; Tashiro, M.; Imada, K.; Kuniyoshi, M. *J. Org. Chem.* **1987**, *52*, 2653–2656.
20. Liu, X.; Kilner, C. A.; Thornton-Pett, M.; Halcrow, M. A. *Acta Crystallogr., Sect. C* **2001**, *57*, 317–318.
21. Ohkawa, S.; DiGiacomo, B.; Larson, D. L.; Takemori, A. E.; Portoghese, P. S. *J. Med. Chem.* **1997**, *40*, 1720–1725. Wang, W.; Li, T.; Attardo, G. *J. Org. Chem.* **1997**, *62*, 6598–6602.
22. Tanzawa, T.; Ichioka, M.; Shirai, N.; Sato, Y. *J. Chem. Soc., Perkin Trans. I* **1995**, 431–436.
23. Farah, B. S.; Gilbert, E. E. *J. Org. Chem.* **1963**, *28*, 2807–2809. Ito, S.; Inoue, S.; Yamamoto, Y.; Fujita, K. *J. Med. Chem.* **1981**, *24*, 673–677. Ranken, P. F.; McKinnie, B. G. *Synthesis* **1984**, 117–119. Hayakawa, K.; Ueyama, K.; Kanematsu, K. *J. Org. Chem.* **1985**, *50*, 1963–1969. Do, Q. T.; Elothmani, D.; Le Guillanton, G. *Tetrahedron Lett.* **1998**, *39*, 4657–4658.
24. Mataka, S.; Mitoma, Y.; Sawada, T.; Thiemann, T.; Taniguchi, M.; Tashiro, M. *Tetrahedron* **1998**, *54*, 5171–5186. Mataka, S.; Shigaki, K.; Sawada, T.; Mitoma, Y.; Taniguchi, M.; Thiemann, T.; Ohga, K.; Egashira, N. *Angew. Chem., Int. Ed. Engl.* **1998**, *37*, 2532–2534.
25. Mataka, S.; Ma, J.; Sawada, T.; Thiemann, T.; Rudzinski, J. M.; Suzuki, H.; Sawada, T.; Tashiro, M. *Tetrahedron* **1997**, *53*, 885–902. Taniguchi, M.; Mataka, S.; Thiemann, T.; Sawada, T.; Mimura, K.; Mitoma, Y. *Bull. Chem. Soc. Jpn* **1998**, *71*, 2661–2668.
26. Simonsen, S. H.; Martin, G. E.; Puig-Torres, S.; Smith, K. *Acta Crystallogr., Sect. C* **1986**, *42*, 766–768. Becker, J. Y.; Bernstein, J.; Bittner, S.; Harlev, E.; Sarma, J. A. R. P. *J. Chem. Soc., Perkin Trans. 2* **1989**, 1157–1160. Song, H.; Kim, E.; Shin, H.-S. *Bull. Kor. Chem. Soc.* **1990**, *11*, 19–21. Holmes, R. R.; Prakasha, T. K.; Day, R. O. *Inorg. Chem.* **1993**, *32*, 4360–4367. Prakasha, T. K.; Day, R. O.; Holmes, R. R. *Inorg. Chem.* **1994**, *33*, 93–98. Larson, S. B.; Schnabelrauch, M.; Vasella, A.; Withers, S. G. *Helv. Chim. Acta* **1994**, *77*, 778–799. Di Vitta, C.; Campos, I. P. deA.; Farah, J. P. S.; Zuckerman-Schpector, J. *J. Chem. Soc., Perkin Trans. I* **2000**, 3692–3694.
27. Thiemann, T.; Ohira, D.; Li, Y.; Sawada, T.; Taniguchi, M.; Yashiro, M.; Mataka, S. *New J. Chem.* **1999**, *23*, 675–678.
28. Mataka, S.; Lee, S. T.; Tamura, Y.; Tsuge, A.; Tashiro, M. *J. Chem. Soc., Perkin Trans. I* **1991**, 1107–1113.
29. Mataka, S.; Mimura, T.; Lee, S. T.; Kobayashi, H.; Yakahashi, K.; Tashiro, M. *J. Org. Chem.* **1989**, *54*, 5237–5241.
30. Cowan, J. A.; Sanders, J. K. M. *J. Chem. Soc., Perkin Trans. I* **1987**, 2395–2402.
31. Stewart, J. J. P. *J. Comput. Chem.* **1989**, *209*, 210–220.
32. Taniguchi, M.; Thiemann, T.; Sawada, T.; Mataka, S. *Z. Anorg. Allg. Chem.* **1999**, *625*, 1249–1251.
33. Jensen, F. *Introduction to Computational Chemistry*; Wiley: Chichester, UK, 1999 pp 84–97.
34. *CS CHEM3D Pro v. 5.0, Program for molecular modelling and analysis*; Cambridge Soft Corporation: Cambridge MA, USA, 1999.
35. Burkuert, U.; Allinger, N. L. *Molecular Mechanics*; American Chemical Society: Washington DC, USA, 1982.
36. *MOPAC 97, Program for semi-empirical calculations*; Fujitsu Ltd: Tokyo, Japan, 1997.
37. Sheldrick, G. M. *Acta Crystallogr., Sect. A* **1990**, *46*, 467–473.
38. Sheldrick, G. M. *SHELXL97, Program for the refinement of crystal structures*; University of Göttingen: Germany, 1997.